3rd European supercritical CO2 Conference
September 19-20, 2019, Paris, France

2019-sCO2.eu-122

HEAT TRANSFER CHARACTERISTICS OF SCO_2 AND DYNAMIC SIMULATION MODEL OF SCO_2 LOOP

Gang Xiao*
Zhejiang University
Hangzhou, China
Email:
xiaogangtianmen@zju.edu.cn

Kaixiang Xing
Zhejiang University
Hangzhou, China

Jinyi Zhang
EDF R&D China
Beijing, China

Yann Le Moullec
EDF R&D China
Beijing, China

Pan Zhou
EDF R&D China
Beijing, China

Tianfeng Yang
Zhejiang University
Hangzhou, China

Mingjiang Ni
Zhejiang University
Hangzhou, China

Kefa Cen
Zhejiang University
Hangzhou, China

ABSTRACT

Supercritical CO_2 (sCO_2) Brayton cycle is a promising power generation technology with high efficiency, compact turbo-machineries and simple layout. Heat exchangers play an important role in sCO_2 Brayton cycle systems. Therefore it is important to have a comprehensive understanding on heat transfer characteristics of sCO_2 at various operation conditions, in order to better design the heat exchangers. A sCO_2 test loop is built to investigate the heat transfer characteristics of sCO_2, which consists of a test section for heat transfer (horizontal straight tube with an inner diameter of 8 mm), an electrical heater of 7.2kW, a heat recuperator of type coil tubes, a back-pressure valve, a CO_2 pump, a CO_2 cooler and a CO_2 storage tank. The test loop is designed to operate with pressure ranging from critical pressure to 15MPa, temperature ranging from critical temperature up to 600 ℃, mass flow rate ranging from 20 to 70kg.h^{-1}. With this test loop, the heat transfer characteristics of sCO_2 under different conditions are measured and studied. These measurements are then used in the development of a new heat transfer correlations for sCO_2. Based on the developed correlation, a dynamic model has been built in Dymola and validated by experimental results. The experimental and simulation results show that: 1) The heat transfer coefficient (HTC) changes greatly for CO_2 at or near the critical point; 2) For sCO_2 at operation conditions far from the critical point, the wall-bulk temperature difference increases between the tube wall and sCO_2 flow with an increasing heating power, and the heat transfer coefficient is relatively stable. The experience gained by the experiment and simulation is then used to design a 150kWe sCO_2 Brayton cycle coupled with a solar solid particle receiver.

INTRODUCTION

Coupled the solar power with the sCO_2 Brayton cycle is one of the promising choices for future power generation. In recent years, many countries have completed the early work for sCO_2 Brayton cycle, such as USA, Korea, China and Japan at el.

The USA, who first suggested to use sCO_2 Brayton cycle in nuclear power system, takes the lead in developing sCO_2 power generation systems. Since 2011, DOE (Department of Energy) of USA started the SunShot Project (65 million dollars invested as research funding) and the Gen 3 Project (72 million dollars invested as research funding) for Supercritical CO_2 power cycle applied in solar thermal system. Sandia National Laboratory (USA) has been implementing and improving a supercritical CO_2 power generation test loop since 2005. Then, a 250kWe re-compression closed Brayton cycle is implemented using two turbine-alternator-compressor units consisting of gas foil bearings.[1] In addition, Bechtel Marine Propulsion Co. developed a 100 kWe supercritical CO_2 power generation cycle test loop using one turbo-generator and one turbo-compressor.[2] Korea Institute of Energy Research developed a 10 kWe-class simple Brayton cycle and an 80 kWe-class test loop for waste heat recovery.[3] Tokyo Institute of Technology (Japan) developed a 100 kWe sCO_2 experimental test loop.[4] Recently, researchers from Southwest Research Institute and General Electric Company (USA) successfully tested the axial sCO_2 turbine at temperature over 700 ℃.

Zhejiang University started the research on sCO_2 power cycle since 2013. In order to have a comprehensive understanding about the heat transfer characteristics of sCO_2 from near ambient temperature to 600 ℃, a test loop was built in 2017. Heat transfer experiments have been carried out in

DOI: 10.17185/duepublico/48881

2018. Based on the test loop, a dynamic model has been developed to explore the dynamic characteristic of a sCO_2 Brayton cycle. The steady state validation of the model has been done, while the dynamic validation with experiments will be finished in next 6 months.

The experience gained by the experiment and simulation is then used to design a 150kWe sCO_2 Brayton cycle coupled with a solar solid particle receiver. The selected cycle design to be implemented is a simple regenerative cycle, with a small-scale turbine and compressor. The inlet temperature and pressure of turbine are set to be 550℃ and 20MPa respectively, and the efficiency of turbine is expected to be over 75%. The inlet temperature and pressure of compressor are set to be 35℃ and 7.4MPa respectively, and the efficiency of compressor is expected to be about 75%. A 2MW regenerator is adopted to increase the compressor outlet sCO_2 flow temperature to 389℃ at 20.1MPa, then with a particle/CO_2 heat exchanger as the main heater, the flow is heated up to 550℃ before entering the turbine. This innovative system is going to be setup in 2019 and demonstrated in 2020 by Zhejiang University, located in a 1MW solar tower.

TEST LOOP IN ZHEJIANG UNIVERSITY

A sCO_2 test loop is developed in Zhejiang University as shown in Figure 1. The CO_2 flow from the gas source passes the filter, and is cooled to liquid phase in the cooling system. The liquid CO_2 flow rate is measured with a flow meter and then pressurized further by the pump. Here, a buffer tank is used to reduce the fluctuation, and a recuperator is used to preheat the liquid CO_2 stream with the exist stream of the sCO_2 from the straight tube test section. Then sCO_2 flow is heated to the designed inlet temperature in the four-stage heater, and flows through the test section. In this section, temperature and pressure of the sCO_2 flow are measured for the heat transfer characteristics investigation. The heat of the sCO_2 flow is reused in the recuperator. Then a heat exchanger is used to further cool down the sCO_2 flow for the safe operation of the back pressure valve. After the pressure is released, sCO_2 flows back to the source. The test loop can offer sCO_2 operating temperature and pressure at 50 ~ 550 ℃, and 8~ 15 MPa respectively at the outlet of the test section.

CO_2 gas (99.99%wt) is used as the working fluid in experiments and the mass flow rate is controlled by a pump whose frequency ranges from 0 to 50 Hz. A mass flowmeter and thermocouples are used. The experiments have been carried out at 20~600 ℃ with the mass flow rate of sCO_2 ranged from 20 to 70 $kg.h^{-1}$ and pressure from 7 to 15 MPa.

HEAT TRANSFER EXPERIMENTS

Heat transfer experiments were carried out for sCO_2 from ambient temperature to 600℃, from 7MPa to 15 MPa. Fig. 2 shows the test section and the locations of the measuring points. The test section was basically a horizontal straight tube with an inner diameter of 8 mm (wall thickness of 3 mm), and it is heated uniformly by a copper column and six heat resistors. The maximum heating power is 7.2 kW. The test section was made of Hac 276 alloy. The horizontal test section was 2.35 m long, and its heated section was 1.75 m. Fifteen K-type thermocouples were attached with 100 mm interval onto the outer surface of the tube to measure the wall temperatures. The test section was heat insulated by insulation cotton. Two pressure sensors and one pressure difference transducer are used to measure the pressure and pressure drop of the inlet and outlet. A straight tube is heated with a maximum heating power of 7.2 kW. Fifteen thermocouples are used to detect outwall temperature along the tube with an interval of 100 mm. The experiments were implemented at steady state. The accuracies and ranges of measuring devices are shown in Table 1. The thermocouples were calibrated by using thermometer, and the maximum error was less than 1.0%. The differences between the corrected value and the thermometer were less than 0.3 ℃ when thermometer readings were between 20 and 100 ℃, respectively. The total uncertainty of the measuring temperature difference is 1.25%. The error in the electric heating power was 4.25%, considering the heat loss. The physical properties of CO_2 were calculated from the NIST package. Based on the calculated formulation, the maximum uncertainty of the heat transfer coefficient was estimated to be ±7.5%.

The tests were conducted with a change of the mass flux and the heat flux at a given pressure. In order to investigate the effects of the pressure on heat transfer, the experiments were carried out at several pressures: 7.6, 8.3, 9 and 11 MPa. Table 2 shows the range of the test conditions. The range of the Reynolds number based on the inlet condition is from 2×10^4 to 1.1×10^5. The working temperature of the test section is controlled from 30 to 600 ℃, which is currently working temperature for the solar receiver.

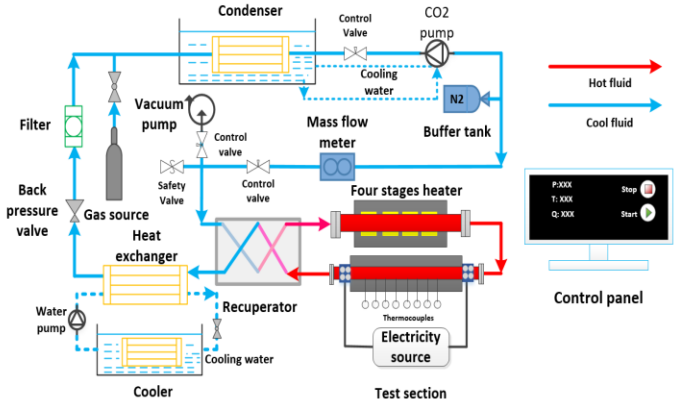

Figure 1: Layout scheme of the Test Loop.

DOI: 10.17185/duepublico/48881

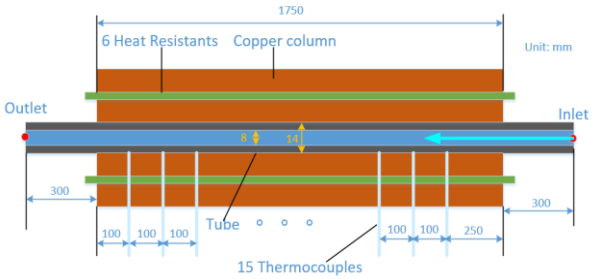

Figure 2: Test section and the locations of the measuring points.

Table 1 Range and accuracy of instruments.

Instruments	Range	Accuracy
Pressure difference transducer	100 kPa	0.1%
	500 kPa	0.1%
	1000 kPa	0.1%
Pressure transducer	10 MPa	0.1%
	25 MPa	0.1%
Thermocouple	220~1440 K	0.75%
Mass flow meter	0~300 hg.h^{-1}	0.2%

Table 2 Parameters of the test conditions.

Fluid	CO_2
Flow direction	Horizontal
Working Pressure (MPa)	7.6, 8.3, 9, 11, 15
Mass flow rate (kg/h)	20-60 kg/h
Inlet temperature, ℃	30~450 ℃
Heat flux q, kW/m^2	0~60
Reynolds number	2×10^4~1.1×10^5

EXPERIMENTAL RESULTS AND DISCUSSION

In Figure 4, several plots are shown for the mass flux from 34 kg/h to 60 kg/h, while the pressure is kept constant at 7.6 MPa, respectively. As the mass flux increases, the peak HTC increases. The HTC reaches the peak value near the pseudo-critical temperature. When fluid temperature (T_b) is higher than 373 K (100 ℃), the HTC is quite stable as shown in Figure 5. As bulk fluid temperature increases, the HTC increases gradually.

Pressure effect is investigated by comparing the test results for 8.3 and 9.1 MPa. In Figure 6, the results show that higher pressure results in lower peak HTC. As the temperature reach the pseudo-critical point, the effect of pressure becomes outstanding, the HTC reach the peak. Especially in the vicinity of the critical pressure, the HTC is several times higher than HTC of conditions far away from pseudo-critical point, due to the steep variation of the physical properties there. In Figure 7, when fluid temperature is higher than 100 ℃, the effect of pressure is not significant. As the pressure increases, the wall temperature decreases.

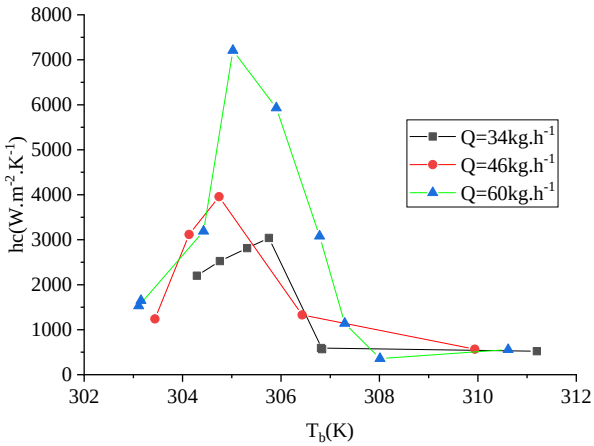

Figure 4: Effect of mass flux on the HTC (pseudo-critical state).

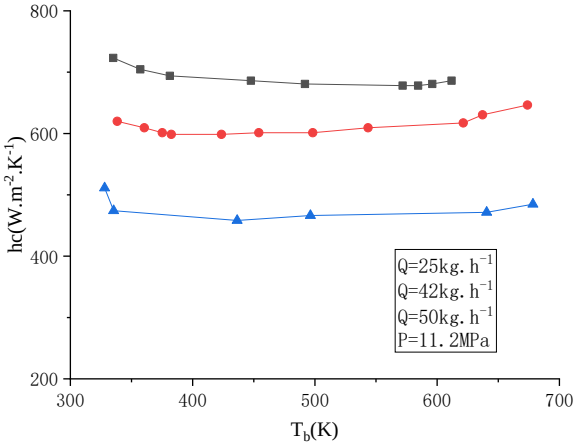

Figure 5: Effect of mass flux on the HTC (high temperature).

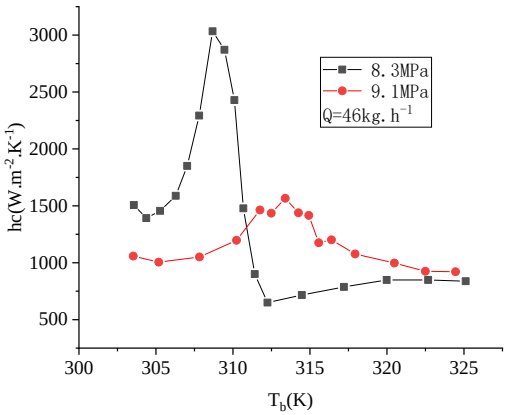

Figure 6: Effect of pressure on HTC (near pseudo-critical temperature).

DOI: 10.17185/duepublico/48881

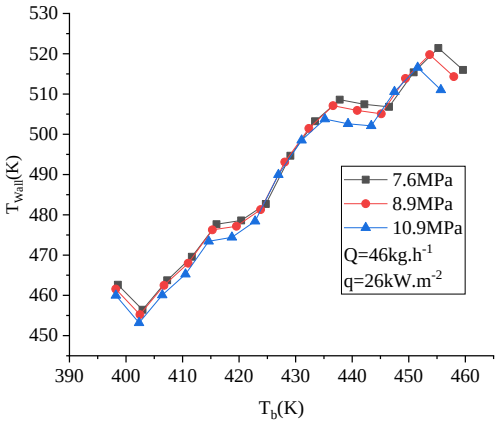

Figure 7: Effect of pressure on the wall temperature.

In order to evaluate the effect of the heat flux, an experiment was performed with the variation of heat flux while keeping the mass flow rate and pressure constant. Figure 8 shows the experimental results for a mass flux of 50 kg/h at a pressure of 11.2 MPa. The wall temperature is plotted along the tube length. The heat flux varies between 0 and 44 kW.m^{-2}. As the heat flux increases, the wall temperature increases. At high temperature, the effect of heat flux is ignorable, as shown in Figure. 9.

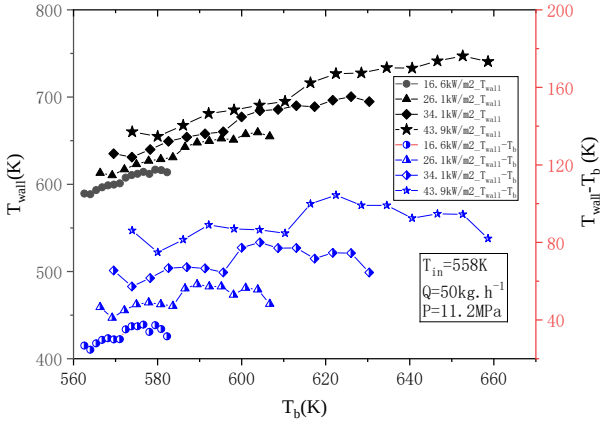

Figure 8: Effect of heat flux on the wall temperature difference.

In the literatures, many equations are available, such as Dittus-Boelte correlation, Gnielinski correlation, Jackson correlation[5], correlation from Liao & Zhao[6, 7], correlation from Kim[8, 9], correlation from Bae[5, 10, 11], et al. However, no correlation is suitable for our test loop experiments. Lee et al.[12] proposed that no simple correlation in terms of traditional dimensional parameters can be expected to give useful predictions except very limited ranges because of the strong coupling of heat transfer and fluid velocity. Here, three equations are used to compare with our experiment results at high temperature range, contains Gnielinski correlation, Dittus-Boelter correlation and Jackson correlation. As shown in Figure 10, at high temperature range, Gnielinski correlation gives better evaluation of the HTC for straight tube than Jackson correlation. The average error between the experiment results and Gnielinski correlation is near 12% (over 20% for Jackson correlation). Near the pseudo-critical temperature (T_{pc}), the Jackson correlation is closer to the experiment result than Gnielinski correlation, as shown in Figure 11. However, the error between experiment results and Jackson correlation is larger than 30%. A new correlation is needed for this working conditions to evaluate the designed test loop.

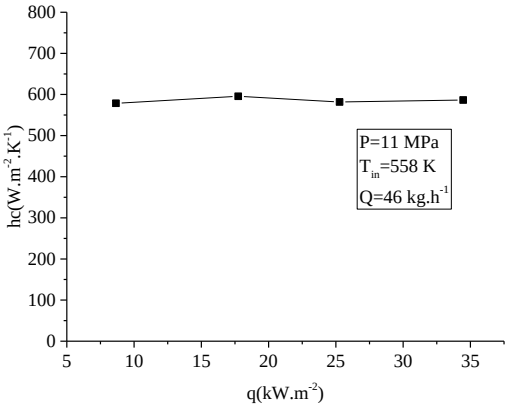

Figure 9: Effect of heat flux on HTC (at high temperature range).

Jackson[5] proposed a friction factor equation contained the Prandtl number, Reynolds number, density ratio and specific heat ratio. The Gnielinski correlation contains Reynolds number, the Prandtl number and the temperature difference facto. To get a better correlation, more factors should be considered. Therefore, the Nusselt number can be represented as a function of the following non-dimensional parameters:

$$Nu = \frac{hcD}{\lambda_{co2}} = f(\mathrm{Re}_b, \mathrm{Pr}_b, \frac{\rho_w}{\rho_b}, \frac{\overline{c_p}}{c_{p,b}}, q^+, c_t) \quad (1.1)$$

$$q^+ = \frac{q\beta_b}{\mathrm{Q}c_{p,b}} \quad (1.2)$$

$$c_t = \frac{T_b}{T_w} \quad (1.3)$$

Where Nu is the Nusselt number, Re is the Reynold number, Pr is the Prandtl number, hc is the THC, λ is the thermal conductivity, c_p is the specific heat, q^+ is the accelerate number, q is the heat flux ratio, c_t is the temperature factor, Q is the mass flux and β_b is volume expansion ratio.

Log-based non-linear curve fitting was employed to correlate the Nusselt numbers from our experiments, and a new heat-transfer correlation was constructed as follows:

DOI: 10.17185/duepublico/48881

$$Nu = 32.39\,\mathrm{Re}_b^{1.0084}\,\mathrm{Pr}_b^{1.9876}\left(\frac{\rho_w}{\rho_b}\right)^{2.2123}\left(\frac{\overline{c_{p,w}}}{c_{p,b}}\right)^{0.7389} q^{+0.9935} c_t^{6.1590} \qquad (1.4)$$

The new correlation gives better result for this working conditions, especially the near the critical point as shown in Figure 13 and 14. The average error of the new correlation is near 5% at high temperature range.

Besides, the present correlation is compared with the Experiment results from Korean Atomic Energy Research Institute (KAERI)[11]. As shown in Fig. 14, the correlation can reflect the difference of HTC better than Dittus-Boelter correlation and Jackson correlation. However, this correlation cannot give a good prediction of the experiment results at that conditions. The mass flow rate and heat flux of the correlation is limited.

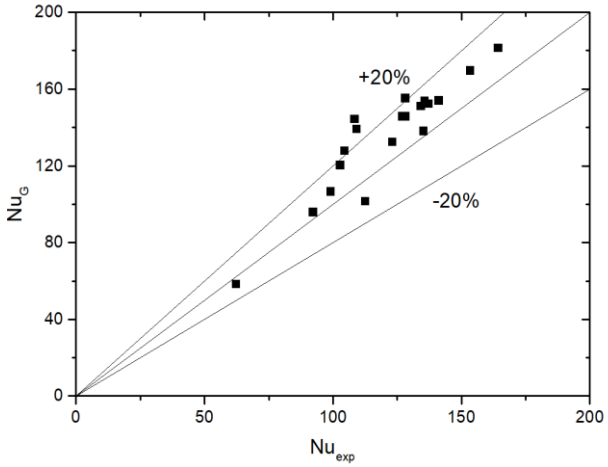

Figure 10: Comparison of HTC (T_b/T_{pc}>1.2) (experiment results and Gnielinski correlation).

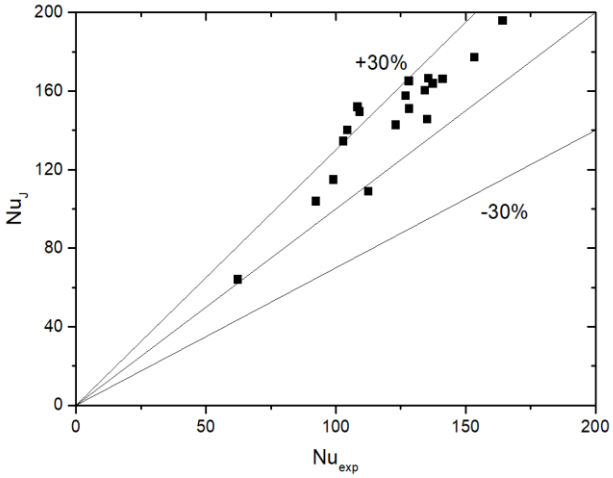

Figure 11: Comparison of HTC (T_b/T_{pc}>1.2) (experiment results and Jackson correlation).

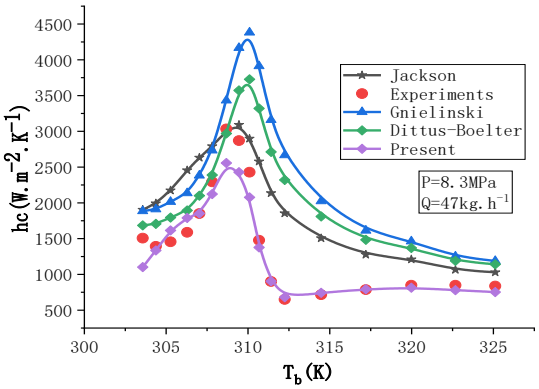

Figure 12: Comparison of HTC at 8.3 MPa (T_b/T_{pc}<1.2) (experiment results, Gnielinski, Dittus-Boelter, Jackson and present correlation).

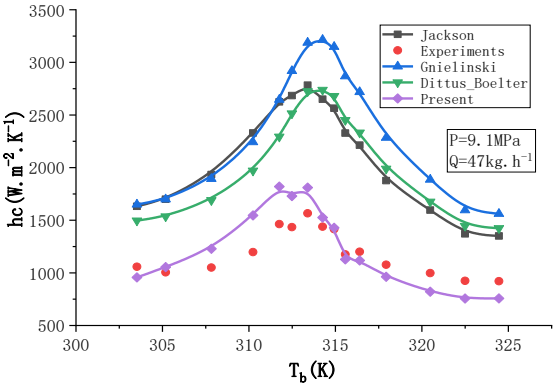

Figure 13: Comparison of HTC at 9.1 MPa (T_b/T_{pc}<1.2) (experiment results, Gnielinski, Dittus-Boelter, Jackson, and present correlation,).

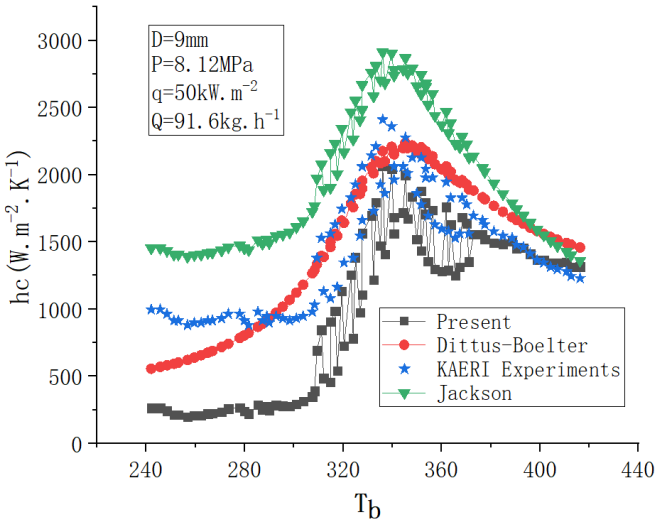

Figure 14: Comparison of HTC data from KAERI (T_b/T_{pc}<1.2) (experiment results, Dittus-Boelter, Jackson, and present correlation,).

DOI: 10.17185/duepublico/48881

DYNAMIC MODEL SIMULATION TOOL

For the sCO_2 Brayton cycle research, a dynamic model is built for this sCO_2 test loop in Dymola Software based on the dynamic modules library ThermoSysPro developed in EDF R&D. The thermodynamic properties of CO_2 is calculated by dynamic calling to NIST REFPROP in real time during simulation. The interface between Dymola and NIST REFPROP is done by MediaTwoPhaseMixture package developed by Henning Francke. The dynamic model is consists of a cooler, a four stages heater, a condenser, a recuperator, a back pressure valve, some control valves, a heating section and a three-plunger pump. In the test loop, back pressure valve is used to replace the turbine, while the friction coefficient change due to the open degree of the valve is regard as the load change during the operation. This dynamic model simulation is used to analyze the dynamic characteristics of different components.

In order to be consistent with the result of the experimental data, some modeling approach is considered. The following assumptions are made for this study:

(1) Pressure losses in the mass flow meter, filter and sensors are replaced by singular pressure loss to reduce the complexity of the loop model for this study;

(2) Expansion process is adiabatic.

(3) Heat loss to the ambient air is estimated by constant heat exchanger coefficient.

(4) The heat conduction between solid media is considered, while the heat conduction within CO_2 is ignored.

DYNAMIC MODEL INTRODUCTION

The pump is used to compress the liquid CO_2 from gas bottle pressure (around 5 MPa) to high working pressure (7~15 MPa) by plunger movement. It uses mechanical work to push the plunger, thus accelerating the liquid. Here we simplified the calculation of pump with constant isentropic efficiency. The relationship between the mass flow rate Q and the pump frequency, pressure ratio P_e is experimentally measured. A map is generated from a steady state situation for a certain temperature, pressure and frequency. The correlations are concluded as follow (according to the pump frequency from 20 to 50):

$$Q = \frac{30.934 - 4.2687Pe}{3600} \quad \text{for frequency=20 HZ} \quad (1.5)$$

$$Q = \frac{45.503 - 5.8544Pe}{3600} \quad \text{for frequency=30 HZ} \quad (1.6)$$

$$Q = \frac{57.802 - 6.21Pe}{3600} \quad \text{for frequency=40 HZ} \quad (1.7)$$

$$Q = \frac{71.459 - 7.21Pe}{3600} \quad \text{for frequency=50 Hz} \quad (1.8)$$

As shown in Figure 15, the correlation concluded for the mass flow rate is closed to the experimental result at different pressure ratios and frequencies. The maximum error of the mass flow correlation is ±1.67%.

We defined the pressure ratio (*Pe*) as:

$$Pe = \frac{P_{in}}{P_{out}} \quad (1.9)$$

Where P_{in} is the pressure at the inlet, P_{out} is the pressure at the outlet.

The isentropic efficiency η is setting as constant (η =0.7) to reducing the model complexity. Then the power can be calculated by equation:

$$W = Q(h_{out} - h_{in}) / (1 - \eta_f) \quad (1.10)$$

Where *h* is the enthalpy, η_f is the friction loss percentage. Here, η_f is 0.1.

The outlet enthalpy of the pump can be calculated by following equations and database:

$$\eta(h_{is} - h_{in}) = h_{out} - h_{in} \quad (1.11)$$

$$s_{out} = s = s_{in} \quad (1.12)$$

Where h_{is} is the isentropic enthalpy at the outlet calculated by the outlet pressure and outlet entropy. Other properties can be calculated by calling REFPROP based the outlet pressure and enthalpy.

Comparison between simulation result and experimental measure value is conducted, and the results are shown in Figure 16. The maximum outlet temperature error is ±1K or ±0.4%, within the measure error of thermocouples (±2.2K or ±0.75%).

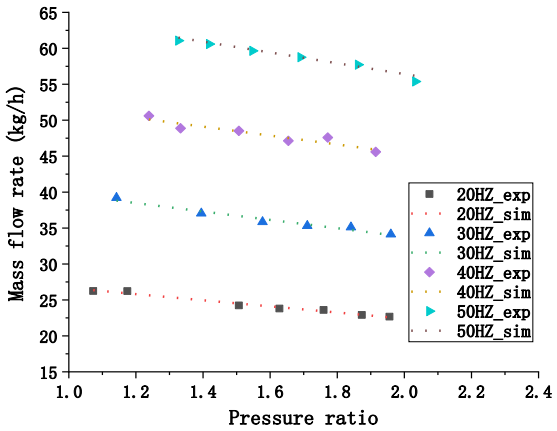

Figure 15: Mass flow map of the three-plunger pump.

Five heat exchangers are utilized in this test loop, including a recuperator, a cooler, a condenser, a four-stage heater and the heat section (test section). These heat exchangers consists of CO_2 pipe and relative wall boundary. The working conditions and pipe geometries are listed in Table 3.

DOI: 10.17185/duepublico/48881

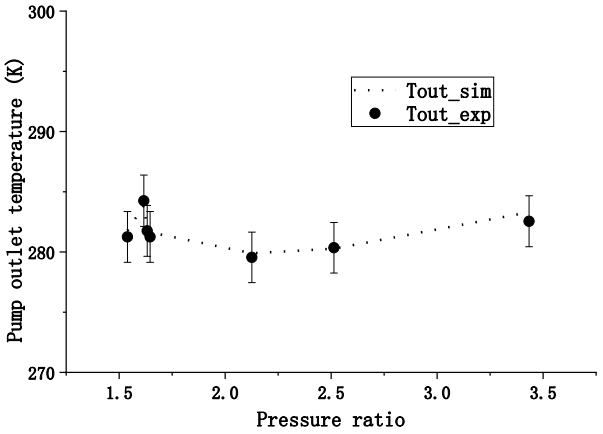

Figure 16: Pump outlet temperature comparison between experiments and simulation (η=0.7).

For a normal pipe, pressure loss equation is simplified as:

$$\Delta P_f = \frac{Q^2}{2\rho} K \tag{1.13}$$

Where K is the pressure drop coefficient, which can be calculated from the experiment results.

The mass flow model and heat transfer model for the dynamic pipe is shown in Figure 17. The dynamic pipe is divided into n sections. Temperature and pressure of each section is assumed uniform.

The energy equation for the fluid can be written as:

$$A(-\frac{dp[i+1]}{dt} + \rho[i].\frac{dh[i+1]}{dt})dx = Q[i].h_b[i] - h_b[i+1].Q[i+1] + dW_1[i] \tag{1.14}$$

Where h_b is the average specific heat capacity of flowing of the fluid, ρ is the density of the fluid, Q is the mass flow rate of the fluid, dW is the heat transfer to the pipe wall. The thermal conduction during two fluid area is ignored.

$$dW_1 = kds[i](Tp[i] - Tw[i]) \tag{1.15}$$

Where, k is the heat transfer coefficient of the CO_2 pipe, ds is the inner wall area per node, and dW1 is calculated by the new correlation (1.2).

$$k = 32.39\,\mathrm{Re}_b[i]^{1.0084}\,\mathrm{Pr}_b[i]^{1.9876}(\frac{\rho_w[i]}{\rho_b[i]})^{2.2123} (\frac{\overline{c_{p,w}[i]}}{c_{p,b}[i]})^{0.7389} q^+[i]^{0.9935} c_t[i]^{6.159} \lambda_{CO2} / D \tag{1.16}$$

$$\mathrm{Re}_b[i] = 4\frac{Q[i]+Q[i+1]}{2.pi.D.\mu_b[i]} \tag{1.17}$$

$$c_t[i] = \frac{T_b[i]}{T_w[i]} \tag{1.18}$$

$$q^+[i] = \frac{qD}{c_{p,b}[i]T_b[i]\mu_b[i]\mathrm{Re}_b[i]} \tag{1.19}$$

Where b means the bulk temperature, w means wall temperature, λ_{CO2} is the thermal conductivity of CO_2, q is the heat flux density, Re is the Reynold number, Pr is the Prandtl number, c_t is the temperature factor and q^+ is the accelerate factor. The properties can be attained from the REFPROP database.

Table 3 Working condition for heat exchangers

Heat exchanger	Pipe diameter Inner/Outer (mm)	Pipe length	Wall condition
recuperator	6/10	12	Normal heat loss to ambient (T_0=15 ℃)
heater	6/10	12×4	Heating power (500W*4) PID control; Normal heat loss to ambient (T_0=15 ℃)
Cooler	4/6	6	Heat loss to cooling water (T_0=0~10 ℃)
Condenser	4/6	12	Heat loss to cooling water (T_0=-5~4 ℃)
Heat section	8/14	2	Heating power (0~7.2 kW); Normal heat loss to ambient (T_0=15 ℃)

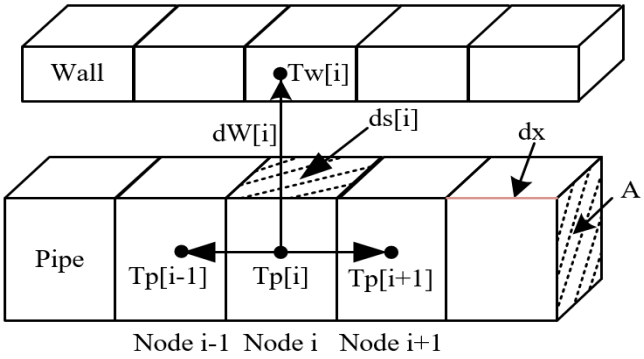

Figure 17: Heat transfer and mass flow model for dynamic pipe.

The mass balance equation for fluid is written as:

$$Adx\{(\frac{d\rho}{dp})_h[i]\frac{dp[i+1]}{dt} + (\frac{d\rho}{dh})_p[i]\frac{dh[i+1]}{dt}\} = Q[i] - Q[i+1] \tag{1.20}$$

The wall is divided into n sections. Temperature and pressure of each section is assumed uniform. The heat transfer model for wall is shown in Figure 18.

The energy equations for solid at node i can be written as:

$$A\rho c_p \frac{dTw[i]}{dt}dx = dW_2[i] + dW_1[i] + A\lambda(2Tw[i] - Tw[i-1] - Tw[i+1])/dx \tag{1.21}$$

DOI: 10.17185/duepublico/48881

Where dW_2 is the energy transferred from the ambient, dW_1 is the energy transferred from the fluid. Thus, in the pipe, the equation of dW_2 and dW_1 are calculated as:

$$dW_2[i] = 2\lambda pi(Tw_2[i] - Tw[i]) / (\log(1 + \frac{e}{e+D}))dx \quad (1.22)$$

$$dW_2[i] = hc(2e + D)pi(T_0 - Tw[i])dx \quad (1.23)$$

$$dW_1[i] = 2\lambda pi(Tw_1[i] - Tw[i]) / (\log(1 + e/D))dx \quad (1.24)$$

Where hc is the heat transfer coefficient between wall and pipe fluid, T_{w1} is the temperature of the wall boundary at the ambient side, T_{w2} is the temperature of the wall boundary at the inner pipe wall side, e is the wall thickness, and D is the inner pipe diameter.

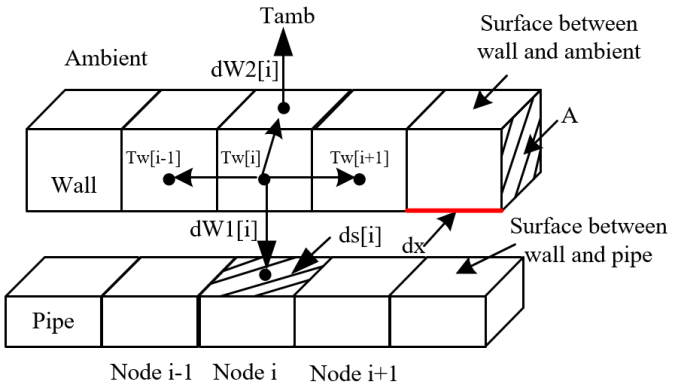

Figure 18: heat transfer model for the heat exchanger wall.

The recuperator is then modelled as two parallel pipes with a wall in between. The condenser and cooler are both modeled with a dynamic pipe and a cooling wall. The test section and four-stage heater are modeled with a dynamic pipe and a heating wall. The models' layout is shown in Figure 19.

The steady state validations of cooler and condenser are performed. The maximum errors of outlet pressure and outlet temperature between simulation and experiments for cooler are separately ±0.1% and ±0.3%, as shown in Figure 20, while the measure errors of the temperature and pressure sensors are separately ±0.75% and ±0.1%. The maximum errors of outlet pressure and outlet temperature between simulation and experiments for condenser are separately ±0.03% and ±0.5%, while the measure errors of the temperature and pressure sensors are separately ±0.75% and ±0.1%.

Validations of the heat section with the experimental results have been conducted for the influence of mass flow rate and working pressure. The maximum error of the outlet temperature and pressure are separately ±1.6% and ±0.2%, as shown in Figure 21.

The back pressure valve is modified from the check valve by setting the pressure loss coefficient. The expanding process in back pressure valve is assumed to be isenthalpic. The pressure loss is calculated by equation (1.11).

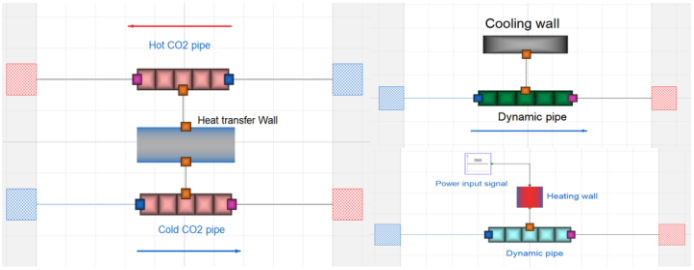

Figure 19: Layout of the heat exchangers: recuperator (left), cooler (right upper) and heater (right down).

The friction factor K is normal working at range between 10^{12} and 10^{14}. The control signal is used to change the friction factor:

$$K = signal.10^{12} \quad (1.25)$$

The signal is at the range of 0.01~100, which means the open degree of the back pressure valve.

Control valve is used to control the fluid in this test loop. The specific enthalpy is assumed constant in the control valve. Here, the pressure drop is calculated by equation:

$$\Delta PCv^2 = K\frac{Q^2}{\rho^2} \quad (1.26)$$

$$\Delta P = P_{out} - P_{in} \quad (1.27)$$

Where Cv is the flow coefficient, which is also used to calculate the pressure drop of the valve. The maximum Cv_{max} is 5000 got from the valve producer. The pressure loss coefficient K is 1.733×10^{12}. Here, actual Cv is calculated as:

$$Cv = Cv_{\max} signal \quad (1.28)$$

The signal here is also used to control the open degree of the valve, while 1 means opening and 0 means closed.

In addition, singular pressure drop model is used to simplify the non-standard pressure drop sections, such as filter and mass flow meter, and is calculated by the equation (1.11). Sensors models are used to get the state in the test loop during simulation.

The complete model is presented in Figure 21. The CO_2 flow from the volume is cooled to liquid phase in the condenser system. The liquid CO_2 flow rate (volumetric) is pressurized further by the pump and then measured with a flow meter. A recuperator is used to preheat the liquid CO_2 stream with the exist stream of the sCO_2 from the Straight Tube Test Section (STTS). Then sCO_2 flow is heated to the designed inlet temperature in the four-stage heater, and flows through the STTS. In this section, temperature and pressure of the sCO_2 flow are measured for the heat transfer characteristics investigation. The heat of the sCO_2 flow is reused in the recuperator. Then a heat exchanger is used to further cool down the sCO_2 flow for the safe operation of the back pressure valve. After released the pressure, sCO_2 flows back to the volume. The steady state validation of the model has been done, while the dynamic validation with experiments will be finished in next 6 months.

DOI: 10.17185/duepublico/48881

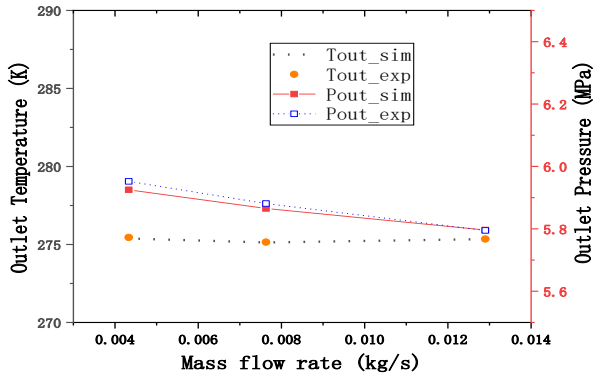

Figure 20: Comparison of the experiment and simulation result for cooler (outlet temperature and pressure).

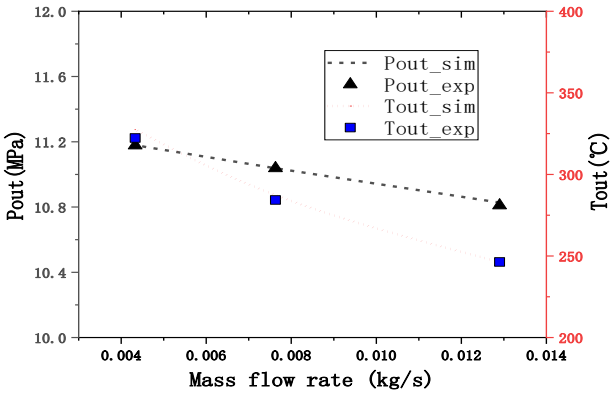

Figure 21: Comparison of the experiment and simulation result for heating section (outlet temperature and pressure).

150KWE SCO_2 BRAYTON CYCLE COUPLED WITH A PARTICLE RECEIVER

The experience gained by the experiment and simulation is then used to design a 150kWe sCO_2 Brayton cycle coupled with a solar solid particle receiver, as shown in Figure 22. The selected cycle design to be implemented is a simple regenerative cycle, with a small-scale turbine and compressor. The inlet temperature and pressure of turbine are set to be 550℃ and 20MPa respectively, and the efficiency of turbine is expected to be over 75%. The inlet temperature and pressure of compressor are set to be 35℃ and 7.4MPa respectively, and the efficiency of compressor is expected to be about 75%. A 2MW regenerator is adopted to increase the compressor outlet sCO_2 flow temperature to 389℃ at 20.1MPa, then with a particle/CO_2 heat exchanger as the main heater, the flow is heated up to 550 ℃ before entering the turbine. This innovative system is going to be setup in 2019 and demonstrated in 2020 by Zhejiang University, located in a 1MW solar tower, as shown in Figure 23.

CONCLUSIONS

Zhejiang University has built a sCO_2 test loop since 2017. The heat transfer experiments have been done. The results show that: (1) existing correlations have significant error near the critical point; (2) at high temperature range, heat transfer characteristics of sCO_2 is quite stable. Base the experimental results, a new correlation is got, and used in the dynamic model developed in Dymola software. The steady state validation has been done. The error between simulation and experiments is smaller than 5%.

Then, in next 6 months, dynamic validation of the model will be completed. And the design experience will be used to design a 150 kWe sCO_2 simple Brayton cycle couple with the 2MW solar tower system built in Zhejiang University. The 150kWe test loop will be constructed in next two years.

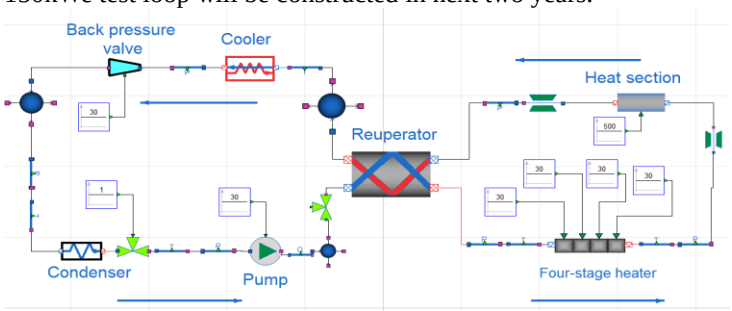

Figure 22: Complete model of the test loop.

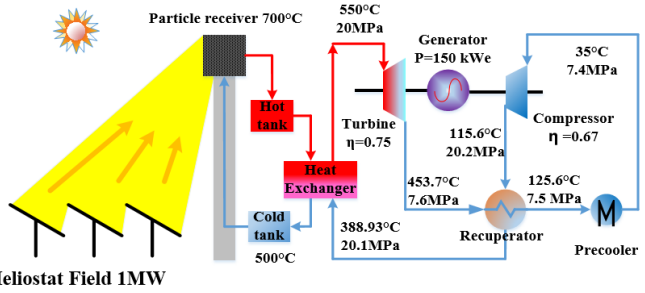

Figure 23: Layout of the 150kWe sCO_2 Brayton cycle.

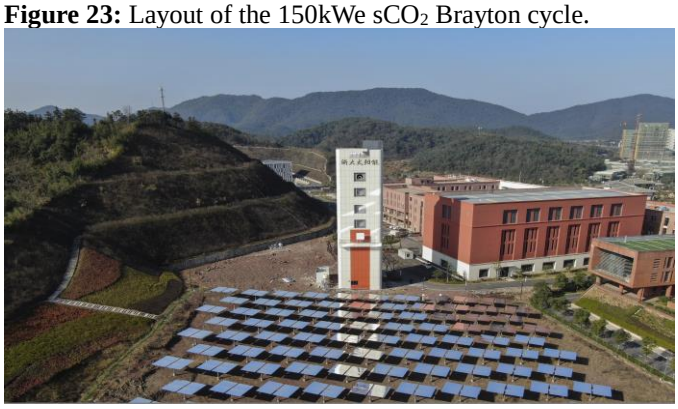

Figure 24: Picture of the 1 MW Solar tower in Zhejiang University.

NOMENCLATURE

A	Area, m^2
Cv	Flow coefficient

DOI: 10.17185/duepublico/48881

c_p	Specific heat, $kJ.kg^{-1}$
c_t	Temperature factor
D	Diameter, m
DOE	Department of Energy
dx	Unit length, m
G	Mass flux, $kg.h^{-1}$
h	Enthalpy, $kJ.kg^{-1}$
hc	Heat transfer coefficient, $W.m^{-2}.K^{-1}$
HTC	Heat transfer coefficient, $W.m^{-2}.K^{-1}$
k	Heat transfer coefficient, $W.m^{-2}.K^{-1}$
K	Pressure drop coefficient
Nu	Nusselt number
P	Pressure
Pe	Pressure ratio
Pr	Prandtl number
q	Heat flux density, $W.m^{-2}$
q^+	Accelerate factor
Q	Mass flow rate, $kg.s^{-1}$
Re	Reynold number
t	Time, s
T	Temperature, K or ℃
W	Power, W
β	Volume expansion ratio, K^{-1}
λ	Thermal conductivity, $W.m^{-2}$
ρ	Density, $kg.m^{-3}$
μ	Dynamic viscosity, $kg.s^{-1}.m^{-1}$
Subscripts and superscripts	
0	Environment
1	Inner face
2	Outer wall face
b	Mass average value
D	Value obtained by Dittus-Boelter correlation
CO_2	Properties of CO_2
exp	Value obtained by experiments
f	Caused by friction
G	Value obtained by Gnielinski correlation
$\overline{h}$	Constant enthalpy
i	Node number
in	Inlet
is	isentropic
J	Value obtained by Jackson correlation
max	Maximum number
$\overline{P}$	Constant pressure
pc	Pseudo-critical
out	Outlet
w	Wall temperature
w1	Inner wall
w2	Outer wall

ACKNOWLEDGEMENTS

This work is supported by National Key Research & Development Program of China (2016YFE0124700).

REFERENCES

[1] Pasch J, Conboy T, Fleming D, Rochau G. Supercritical CO2 Recompression Brayton Cycle: Completed Assembly Description. Sandia; 2012.

[2] Cho J, Choi M, Baik Y-J, Lee G, Ra H-S, Kim B, et al. Development of the turbomachinery for the supercritical carbon dioxide power cycle. International Journal of Energy Research. 2016;40:587-99.

[3] Cho J, Shin H-K, Ra H-S, Lee G, Roh C, Lee B, et al. Research on the development of a small-scale supercritical carbon dioxide power experimental test loop. The 5th International Symposium - Supercritical CO2 Power Cycles. San Antonio, Texas2016.

[4] Utamura M, Hasuike H, Ogawa K, Yamamoto T, Fukushima T, Watanabe T, et al. Demonstration of Supercritical CO2 Closed Regenerative Brayton Cycle in a Bench Scale Experiment. 2012:155-64.

[5] Bae YY. Mixed convection heat transfer to carbon dioxide flowing upward and downward in a vertical tube and an annular channel. Nuclear Engineering and Design. 2011;241:3164-77.

[6] Liao SM, Zhao TS. Measurements of Heat Transfer Coefficients From Supercritical Carbon Dioxide Flowing in Horizontal Mini/Micro Channels. Journal of Heat Transfer. 2002;124:413.

[7] Liao SM, Zhao TS. An experimental investigation of convection heat transfer to supercritical carbon dioxide in miniature tubes. International Journal of Heat and Mass Transfer. 2002;45:5025-34.

[8] Kim H, Kim HY, Song JH, Bae YY. Heat transfer to supercritical pressure carbon dioxide flowing upward through tubes and a narrow annulus passage. Progress in Nuclear Energy. 2008;50:518-25.

[9] Kim DE, Kim M-H. Experimental investigation of heat transfer in vertical upward and downward supercritical CO2 flow in a circular tube. International Journal of Heat and Fluid Flow. 2011;32:176-91.

[10] Bae Y-Y, Kim H-Y, Kang D-J. Forced and mixed convection heat transfer to supercritical CO2 vertically flowing in a uniformly-heated circular tube. Experimental Thermal and Fluid Science. 2010;34:1295-308.

[11] Bae Y-Y, Kim H-Y. Convective heat transfer to CO2 at a supercritical pressure flowing vertically upward in tubes and an annular channel. Experimental Thermal and Fluid Science. 2009;33:329-39.

[12] Lee SH, Howell JR. Turbulent developing convective heat transfer in a tube for fluids near the critical point. Int J Heat Mass Transfer. 1998;41:14.

 DOI: 10.17185/duepublico/48881

DOI: 10.17185/duepublico/48881
URN: urn:nbn:de:hbz:464-20191004-130154-6